Hole transport in the organic small molecule material α-NPD : evidence for the presence of correlated disorder

Hole transport in the organic small molecule material α-NPD: evidence for the presence of correlated disorder

S. L. M. van Mensfoort,[1,2,a)] V. Shabro,[2] R. J. de Vries,[1,2] R. A. J. Janssen,[1] and R. Coehoorn[1,2]

[1]*Molecular Materials and Nanosystems, Department of Applied Physics, Eindhoven University of Technology, P.O. Box 513, 5600 MB Eindhoven, The Netherlands*

[2]*Philips Research Laboratories, High Tech Campus 4, 5656 AE Eindhoven, The Netherlands*

(Received 8 January 2010; accepted 24 March 2010; published online 9 June 2010)

In this paper the hole mobility in the amorphous small molecule material N,N′-bis(1-naphthyl)-N,N′-diphenyl-1,1′-biphenyl-4,4′-diamine (α-NPD), which is frequently used in organic light-emitting diodes, is studied. From an analysis of the temperature and layer thickness dependence of the steady-state current density in sandwich-type α-NPD-based hole-only devices, it is found that a conventional mobility model assuming a Poole–Frenkel type field dependence and neglecting the carrier density dependence is not appropriate. Consistent descriptions with equal quality are obtained within the framework of two forms of the Gaussian disorder model (GDM and CDM), within which the presence of energetic disorder is described by a Gaussian density of states and within which spatial correlations between the site energies are absent or are included, respectively. Both models contain a carrier density dependence of the mobility. Based on a comparison of the site densities as obtained from both models with the molecular density, we argue that the analysis provides evidence for the presence of correlated disorder. © *2010 American Institute of Physics*. [doi:10.1063/1.3407561]

I. INTRODUCTION

The most efficient white organic light-emitting diodes (OLEDs) that are currently produced in research laboratories are multilayer devices based on small molecule organic semiconductors.[1–4] The approach toward optimizing the efficiency and lifetime is based on the introduction of novel layer structure concepts as well as novel organic materials, followed by empirical optimization. This usually involves making many devices, varying the layer thicknesses of the individual layers in a trial-and-error process. Subsequently, the most promising device structures are selected on the basis of the results from current-voltage-luminance measurements. Advances in the understanding of how the current density and the charge carrier distribution in each layer depend on the layer structure and thicknesses and on the applied voltage would help considerably to build up a predictive OLED device model that allows one to rationally design OLEDs with increased performance.[5]

For developing a predictive OLED device model it is crucial to understand the effects of energetic disorder on the charge transport in the small molecule materials used, in particular how the mobility, μ, depends on the temperature, T, the electric field, F, and the charge carrier density, p.[6] Frequently, the disorder is described by assuming a spatially uncorrelated Gaussian energy distribution (Gaussian Disorder Model, GDM).[7] The shape of the density of states (DOS) is described by its width, σ, and the transport site density, N_t. For the GDM, expressions for the mobility function have been obtained from semianalytical,[8–12] three-dimensional master equation (3D-ME),[13] and Monte Carlo calculations.[7,14] In a limited field range, the field dependence of the mobility is then well described by the Poole–Frenkel (PF) type expression $\mu(F) \propto \exp(\gamma\sqrt{F})$,[15,16] which is used more conventionally in analyzes of transport in OLEDs. Here, γ is a parameter that describes the strength of the field dependence. Alternatively, the disorder is often described by assuming a *spatially correlated* Gaussian energy distribution (correlated disorder model, CDM), resulting from charge-dipole interactions. A PF-type field dependence is then already found at smaller fields than in the GDM, which has been argued to be in better correspondence with experiments.[17,18] Recently, Bouhassoune *et al.* have obtained the F and p dependence of the mobility as a function of the energetic disorder within the CDM, using 3D-ME calculations.[19,20] For small but realistic electric fields, the field dependence of the mobility is within the CDM much stronger than within the GDM.[19] On the other hand, the charge carrier density dependence is for the CDM slightly weaker.[19]

Although accurate theoretical descriptions of the charge transport are thus available for the two frequently used disorder models discussed above, their applicability to disordered *small-molecule* materials, as used in today's most efficient OLEDs, has not yet been fully established. More specifically, for developing a predictive OLED device model it is crucial to be able to make a distinction between spatially correlated and uncorrelated disorder. Such analyzes have so far only been made for certain *polymers*, as discussed in more detail below. Analyzes of charge transport in small molecule materials, carried out in the framework of the GDM and the CDM but neglecting the charge carrier density dependence, led to $\sigma \approx 0.08-0.15$ eV for commonly used

a)Electronic mail: siebe.van.mensfoort@philips.com.

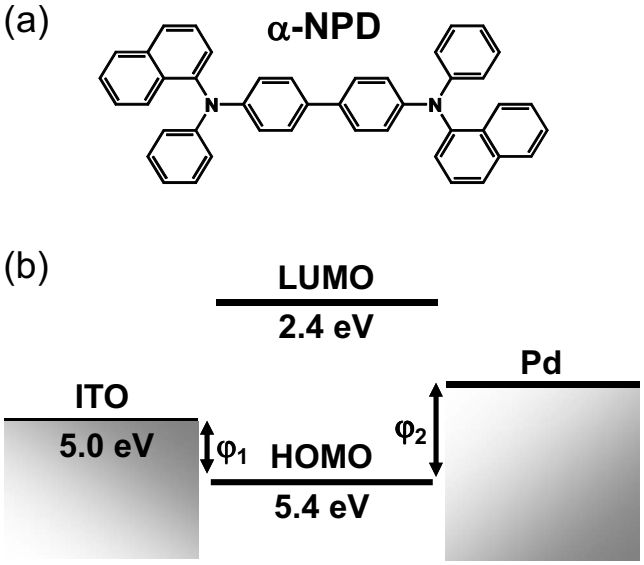

FIG. 1. Chemical structure of the α-NPD molecule (a) and schematic energy diagram of the glass $|$ITO$|\alpha$-NPD$|$Pd structures as obtained from this study, indicating the hole injection barriers at the anode (ϕ_1) and at the cathode (ϕ_2), and the HOMO and LUMO energies of α-NPD (b). The (effective) work functions of ITO and Pd in this system are discussed in the text.

OLED materials.[21–25] Neglecting the charge carrier density dependence can be appropriate for the case of injection-limited transport, in devices with large injection barriers. However, in the absence of large injection barriers the charge carrier density dependence of the mobility and its effect on the current density cannot be neglected. For materials with a Gaussian DOS with $\sigma \approx 0.1$ eV, the effect is theoretically expected to become significant for carrier concentrations (site occupation probabilities) larger than approximately 10^{-4} at room temperature. The occurence of such a cross-over concentration and the relevance to OLED device modeling have first been established experimentally for poly(p-phenylene-vinylene) (PPV) based systems.[26] Including the carrier density dependence of the mobility in the analysis of transport measurements would therefore be needed to establish the actual applicability of the GDM or CDM, and to resolve controversies concerning the presence and degree of the spatial correlation of the site energies. For example, Malliaras *et al.*[21] argued that in the frequently used small molecule material tris(8-quinolinolato)aluminum (Alq_3) the site energies are correlated, using an analysis of time-of-flight experiments. On the other hand, Nagata and Lennartz[27] suggest that the site energies in Alq_3 are not strongly correlated and that the mobility can be quite strongly carrier density dependent as result of the disorder, using the results of a recent combined molecular dynamics and Monte Carlo simulation study.

In this paper, the possible presence of correlated disorder and its effect on the hole transport are investigated for the archetypical small molecule material [N,N′-bis(1-naphthyl)-N,N′-diphenyl-1,1′-biphenyl-4,4′-diamine] (α-NPD). This material [also called NPB, see Fig. 1(a)] is widely used in OLEDs as a hole-injection layer,[28] hole-transport layer,[29–34] electron-blocking layer,[35] blue-emitting layer,[36,37] and as a host material in mixed emitting layers.[31,38–40] The relatively high glass transition temperature, 95 °C, is viewed as beneficial to the OLED stability. In none of the earlier studies of the hole-mobility of α-NPD, based on the steady-state current density versus voltage [$J(V)$] curves,[16,24,41,42] time-of-flight measurements[43–49] or impedance measurements,[50] the carrier-density dependence of the mobility was taken into account.

We analyze temperature-dependent experimental $J(V)$ curves of sandwich-type hole-only devices for two thicknesses of the α-NPD layer. As a first step, we show that the thickness dependence of the $J(V)$ curves cannot be described consistently using the conventional mobility model with the PF-type field dependent mobility function. Subsequently, we show that using a mobility model that takes the carrier density and field dependence of the mobility into account in the framework of the GDM, a fully consistent description of the thickness, temperature and voltage dependence of the current density can be obtained. However, in order to describe the data, a hopping transport site density N_t has to be assumed that is much smaller than the volume density of α-NPD molecules. As a third step, we investigate to what extent the CDM can consistently describe the experimental data. We find that an equally good fit to the $J(V)$ curves can be obtained as within the GDM, and with a value of N_t close to the molecular density. This finding suggests that in α-NPD site-energy correlations do play a role. We note that the application of a similar approach to several types of *polymers*, including well-known PPV-derivatives[13] and a blue-emitting polyfluorene-based copolymer,[51] led to the opposite conclusion: their mobility is described well using the GDM, and no evidence for the presence of spatial correlation was found.[19,52]

In Sec. II the sample preparation and measurement techniques are outlined, and the measured $J(V)$ curves are presented. Section III discusses the analysis of the curves using the conventional mobility model, using the GDM and using the CDM. In Sec. IV, the model parameters that optimally describe the experimental results are critically discussed and possible origins of site-energy correlations in small molecules are presented. Section V contains a summary and conclusions.

II. EXPERIMENT

The devices used to study the hole transport in α-NPD have the following structure:

Glass|ITO|α-NPD|Pd,

with a 100 nm indium tin oxide (ITO) anode, a 100–200 nm α-NPD layer, and a ~100 nm palladium cathode layer. The glass substrates with patterned ITO are exposed to UV/ozone prior to the deposition of α-NPD. The α-NPD layer and the Pd layer are deposited by evaporation in a high-vacuum system with a substrate temperature of ~295 K. The thicknesses of the deposited layers are monitored during deposition using a calibrated resonance crystal. Two series of samples are investigated in this study: one series with a thickness $L=100$ nm of the α-NPD layer and one series with $L=200$ nm. For each thickness 27 nominally identical

3×3 mm^2 devices were prepared on a single substrate. To protect the devices from water and oxygen contamination, the devices were encapsulated using a metal lid enclosing a desiccant getter. A diagram schematically indicating the energy level alignment in the devices studied, found from the analysis presented below, is shown in Fig. 1(b). The highest occupied molecular orbital (HOMO) and lowest unoccupied molecular orbital (LUMO) energies of α-NPD are reported to be ~5.4–5.6 eV and ~2.3–2.7 eV, respectively.[53,54] From the nominal (vacuum) work function of ITO (~4.7–5.0 eV, depending on the cleaning treatment) the barrier for hole injection at the anode interface, ϕ_1, is therefore estimated to be 0.4–0.9 eV. From the nominal work function of palladium (~5 eV) the barrier for electron injection would be expected to be at least 2.3 eV. However, from the analysis we will show that the effective value is smaller, but that still the barrier for electron injection will be larger than 1 eV, large enough to suppress electron injection to a negligible level. Indeed, no light emission was observed from the devices up to the highest voltages applied in this study.

Four-point impedance spectroscopy measurements were performed using a Schlumberger SI-1260 impedance/gain-phase analyzer to determine the voltage-dependent differential capacitance (C) of the diodes at low frequencies (f). The $C(V)$ curves show a small narrow peak in the differential capacitance at 1.3 ± 0.1 V, with a height that is ~6% larger than the geometrical capacitance, C_{geom}. In Ref. 55 it was shown that for the case of a device with a well-injecting contact for holes at the anode and a high injection barrier for holes and electrons at the cathode, the height of the peak is expected to be $1.42\times C_{\mathrm{geom}}$. In line with the results presented in Ref. 55 we conclude from the observation of the (small) peak that the ITO$|\alpha$-NPD interface does not form a perfectly Ohmic contact (so that $\phi_1>0$ eV), but that it also does not strongly limit the hole injection (ϕ_1 at most a few tenths of an electron volt). As a consequence, the built-in voltage (V_{bi}) is expected to be slightly larger than 1.3 V.

From our analysis in Sec. III, we find $\phi_1=0.4\pm0.1$ eV and $V_{\mathrm{bi}}\equiv(\phi_2-\phi_1)/e=1.5\pm0.1$ V, with e the elementary charge, consistent with the rough estimate given above from the $C(V)$ results. In Fig. 1 the highest and the lowest reported values for the effective Fermi energy of ITO and the HOMO level of α-NPD are taken, respectively, in order to get a consistent description of the injection barrier at this interface. The values of ϕ_1 and V_{bi} obtained from our analysis result in an estimated value of $\phi_2=1.9\pm0.2$ eV. This would yield an effective Fermi energy of ~3.5 eV for the Pd cathode in contact with α-NPD, whereas the vacuum work function of polycrystalline Pd is approximately 5.1 V. The result is consistently found for all layer thicknesses and temperatures, as discussed in Sec. III B. The effective interface dipole energy is thus remarkably large, viz., 1.6 eV. However, we note that an even slightly larger interface dipole energy, ≈2.0 eV, was found for interfaces of Pd on top of another amine-containing organic semiconductor, viz., a polyfluorene-based copolymer containing triarylamine hole transporting units.[51,52] For α-NPD on top of Au the effect is ≈1.15 eV,[56] and similarly large interface dipole energies have been observed for many other systems.[57–59]

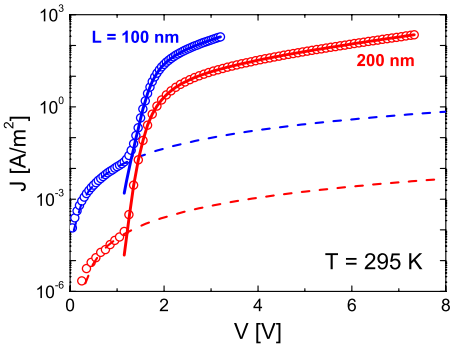

FIG. 2. (Color online) Experimental current density vs voltage curves for a 100 nm and a 200 nm α-NPD sample at room temperature (symbols). The data points of the 200 nm device are displaced by +0.2 V in order to prevent overlap with the data points of the 100 nm device. The dashed curves are extrapolated linear fits to the data for $V<1$ V. The thick full curves are the experimental data after subtraction of this "leakage" current contribution.

Current density versus voltage curves were measured for the hole-only devices as a function of temperature, with T in the range of 160–295 K. Figure 2 shows examples of the $J(V)$ curves for a 100 nm device and a 200 nm device at room temperature (symbols). Also shown in the figure are linear fits to the $J(V)$ curves at low voltages ($V<1$ V), extrapolated to larger voltages (dashed curves). This is viewed as a leakage current density, as discussed in Ref. 55. The thick full curves represent the current density after subtraction of this leakage current contribution. All experimental $J(V)$ curves presented in the remainder of this paper have been corrected for a linear leakage current contribution. In Sec. III, it is investigated to what extent the $J(V)$ curves can be described using the conventional mobility model, using the GDM, and using the CDM. In order to assess the validity of the GDM and of the CDM, the density of transport sites, N_{t}, is used as a discriminating factor. From the molar mass of α-NPD (588.7 g/mol) and the experimentally determined density of α-NPD in the crystalline phase (1.223×10^3 kg/m^3), N_{t} is estimated to be 1.25×10^{27} m^{-3}. In a deposited thin organic film, deviations from the bulk density might occur. From inductively coupled plasma atomic emission spectrometry (ICP-AES) (Ref. 60) measurements on α-NPD coated silicon substrates, we have obtained a molecule volume density of $(1.4\pm0.1)\times10^{27}$ m^{-3}, using carbon detection.

III. ANALYSIS OF $J(V)$ CURVES

A. Analysis assuming a PF type mobility function

As already described in Ref. 51, conventionally charge transport in disordered organic semiconductors is analyzed in terms of a mobility with a PF-type electric field (F) dependence of the form

$$\mu(F,T) = \mu_0(T)\exp(\gamma(T)\sqrt{F}), \tag{1}$$

with γ the field activation factor and μ_0 the mobility in the limit of zero field. Empirically, the temperature dependence of μ_0 and γ is often found to be well described by[61]

$$\mu_0(T) = \mu_0^* \exp\left(-\frac{\Delta}{k_B T}\right), \quad \text{and} \tag{2}$$

$$\gamma(T) = \beta\left(\frac{1}{k_B T} - \frac{1}{k_B T_0}\right), \tag{3}$$

where μ_0^*, Δ, β, and T_0 are parameters that can be determined from experiments. The mobility μ_0^* can be viewed as the mobility in the limit of zero field and infinite temperature and Δ is an effective activation energy.

Using Eq. (1), $J(V)$ curves are calculated employing the drift-diffusion device model introduced in Ref. 62. The site density, which in this case only affects the hole density boundary conditions, is fixed to the experimental value, 1.4×10^{27} m^{-3}. Variations in N_t of a factor 2 were found to have no effect on the quality of the fit to the data using the conventional model. The introduction of a hole injection barrier at the ITO|α-NPD interface affects the analysis negatively, in the sense that the discrepancies concerning the thickness dependence of the hole transport, discussed below, increase. Therefore, ϕ_1 is taken equal to zero. The results discussed below therefore represent the best possible description of the hole transport in α-NPD within the framework of the conventional model. For the relative permittivity (ε_r) we use a value of 3.8. The sensitivity of the analysis of $J(V)$ curves to variations in the chosen value of ε_r was verified. It is found that for ε_r in the range of 2.8–4.8 there is no significant change in the quality of the description of the experimental data provided by the model, nor in the values of the optimized parameters, except for a change in the mobility values obtained. A change of ε_r from 3.8 to 2.8 (4.8) was found to lead to an increase (decrease) of the mobility values obtained of at most 25%, depending on the layer thickness and temperature.

First, the parameters μ_0^*, Δ, β, and T_0 were optimized for the temperature dependent $J(V)$ results obtained for the $L = 200$ nm devices. The resulting $J(V)$ curves are presented in Fig. 3(a). An excellent description of the curves is obtained using the following approach. Starting at room temperature, a $J(V)$ curve is calculated for an initial choice of γ. The fit of this calculated curve to the experimental curve at this temperature is optimized by varying ϕ_2 and $\mu_0(T)$. To a very good approximation, this leaves the shape of the calculated $J(V)$ curve on a log(J) versus V scale unchanged, but only determines the position of the curve. As a next step the error, which is taken as the normalized root-mean-square distance between the calculated and the measured $J(V)$ curve,[63] is minimized by optimizing the value of γ. The procedure is then repeated for all other temperatures for which experimental $J(V)$ curves were obtained. The built-in voltage, which is in this case equal to ϕ_2/e, is found to be equal to 1.4 ± 0.1 V for all temperatures.

Figure 4 shows the values of $\gamma(T)$ obtained in this way. The parameters β and T_0 are obtained from a fit to the $\gamma(T)$ values using Eq. (3). We find $\beta = (4.7 \pm 0.3) \times 10^{-5}$ eV$(m/V)^{1/2}$ and $T_0 = 310 \pm 30$ K. The calculated $J(V)$ curves presented in Fig. 3(a) for the 200 nm device are obtained using $\gamma(T)$ values from the linear fit, therefore making use of a slightly improved statistics. The corresponding values of $\mu_0(T)$ are also shown in Fig. 4 and are well described by Eq. (2) for $\Delta = 0.488 \pm 0.08$ eV and $\mu_0^* = 0.2 \pm 0.1$ m^2/V s. For the zero-field mobility at room temperature we find a value of $\sim 1 \times 10^{-9}$ m^2/V s, at the lower boundary of the values in the range of 10^{-9}–10^{-6} m^2/V s reported in the literature.[16,24,41–50] The results obtained for β, T_0, and Δ are very similar to the values reported in Ref. 64 and references therein, for a PPV-derivative, which one

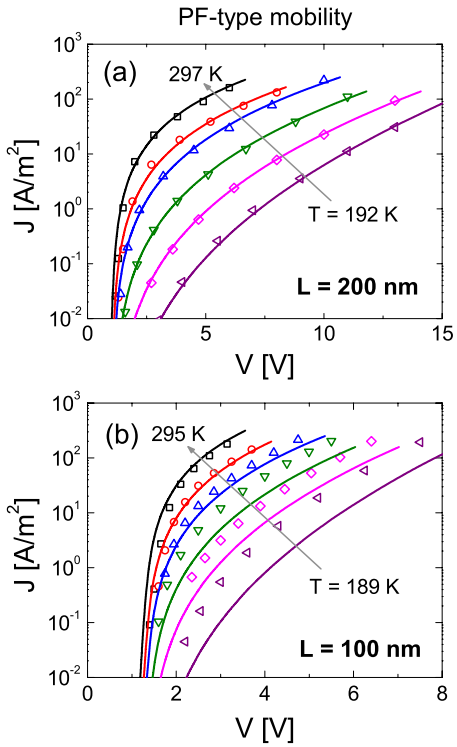

FIG. 3. (Color online) Measured (symbols) and calculated (curves) $J(V)$ curves for a 200 nm α-NPD hole only device at 297, 273, 254, 232, 213, and 192 K (a) and for a 100 nm device at 295, 272, 255, 233, 215, and 189 K (b), as a function of temperature. The calculations are performed using a drift-diffusion device model, assuming a conventional field-dependence of the mobility, with parameters optimized for the 200 nm device.

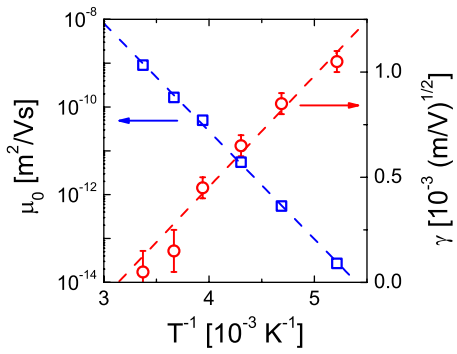

FIG. 4. (Color online) Conventional PF-type mobility model parameters γ (circles) and μ_0 (squares) as a function of $1/T$ for the 200 nm device, for which the $J(V)$ curves are shown in Fig. 3. The dashed lines are fits using Eqs. (2) and (3).

could view as an indication that the physics governing hole transport in small molecule materials and in polymers is not necessarily different. However, we note that the value of μ_0^* is two orders of magnitude larger than the values in the range of 0.003–0.004 $m^2/V\,s$ obtained by Craciun *et al.*[65] from a similar analysis for a large number of polymers.

The parameter values mentioned above, obtained from an analysis of the $L=200$ nm data, were used to predict the $J(V)$ curves of the 100 nm devices. The results are shown in Fig. 3(b). At the highest two temperatures, the calculated $J(V)$ curves differ only slightly from the measurement results. However, at lower temperatures the predictions strongly underestimate the experimental current density, up to approximately one order of magnitude for the lowest temperatures. We have also found that a parameter set that seeks to describe the data of both thicknesses simultaneously, and which is therefore a compromise, leads to unsatisfactory results for both thicknesses (not shown). From these results we conclude that it is not possible to consistently describe the temperature and layer thickness dependent hole transport in α-NPD using the conventional mobility model as described by Eq. (1).

B. Analysis assuming transport in a Gaussian DOS

In this subsection, we analyze the $J(V)$ curves assuming transport in a Gaussian DOS, using the GDM and the CDM. In both models the mobility functions can be expressed as

$$\mu(p,F,T) = \mu_0(T) f(p,F,T), \tag{4}$$

with μ_0 the temperature-dependent mobility in the zero field and carrier density limit and with $f(p,F,T)$ a dimensionless function that depends on N_t and σ for both the GDM and the CDM. Site energy correlations in disordered organic semiconductors can have various origins. They can, e.g., be the result of interaction of charges with randomly oriented dipoles,[17,18] and of a variable morphology.[66] In polymer systems, they can also be caused by a variable molecular geometry.[67] We make use of the mobility functions as calculated in Ref. 19, where correlated disorder due to randomly oriented dipoles is assumed. This approach leads to a value of σ which is proportional to the dipole moment.[17,68] No new parameter, such as a correlation length, is introduced. The pair correlation function of the site energies decreases by a factor of 2 within approximately 1.5 average intersite distances, and has at larger distances (r) an algebraic ($1/r$) form.[18,19] When employing the CDM we are therefore addressing the question whether site-energy correlations with this specific correlation function are present in α-NPD. Whether these correlations are in fact the result of random dipoles or have another origin would then still be an open question. Within the CDM the carrier density (p) and field dependence of the mobility, as described by the function $f_{CDM}(p,F,T)$ given in Ref. 19, are smaller and larger, respectively, than within the GDM, for which the function $f_{GDM}(p,F,T)$ is given in Ref. 13.

In contrast to the analysis using the conventional mobility model, it is found upon analyzing the experimental $J(V)$ curves using the GDM and using the CDM that the inclusion of an injection barrier at the ITO|α-NPD interface significantly improves the correspondence between experiment and model. We assume that the effective barrier height $\phi_{1,eff}$ for injection is determined by the nominal barrier height ϕ_1, defined as the energy difference between the HOMO level of α-NPD and the Fermi-level of the ITO anode, reduced due to the image charge potential and the electric field at the interface.[69] The carrier density boundary condition is then obtained by assuming local thermal equilibrium at the interface.

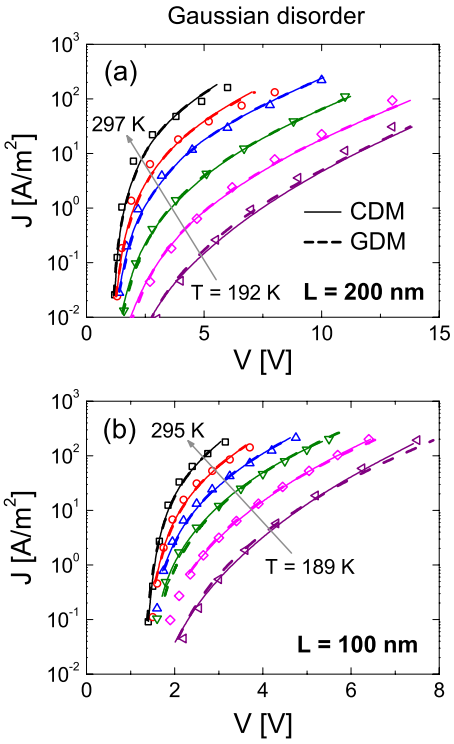

FIG. 5. (Color online) Measured (symbols) and calculated (dotted and dashed curves) $J(V)$ curves for a 200 nm α-NPD hole only device (a) and for a 100 nm device (b), as a function of temperature. The calculations are performed assuming a carrier-density and field-dependent mobility following from the GDM (dotted curves) and from the CDM (dashed curves). The relevant parameters are discussed in the text.

Figure 5 shows optimal fits to the experimental $J(V)$ data for the GDM (full curves) and for the CDM (dashed curves). For both the GDM and the CDM an excellent description of the full thickness, temperature, and voltage dependence of the current density is obtained. The *shape* of the $J(V)$ curves depends on only two temperature and thickness-independent material parameters, N_t and σ, and on one device parameter, ϕ_1. For the GDM, we find $N_t=(2.0\pm0.4)\times10^{26}$ m^{-3} and $\sigma=0.14\pm0.01$ eV, and for the CDM $N_t=(3.7\pm0.8)\times10^{27}$ m^{-3} and $\sigma=0.10\pm0.01$ eV. By optimizing the *position* of the $J(V)$ curves, using a shift along the horizontal and vertical axes, one (temperature independent) value of ϕ_2 and temperature dependent optimal values of μ_0 are determined. Both for the GDM and for the CDM we find $\phi_1=0.4\pm0.1$ eV and $\phi_2=1.9\pm0.1$ eV, leading to $V_{bi}\approx1.5$ V. The consistency of the procedure follows from the observation (see Fig. 6) that the temperature-dependent values of μ_0 differ less than a factor 1.5 for the two layer thicknesses considered. The built-in voltage is remarkably high,

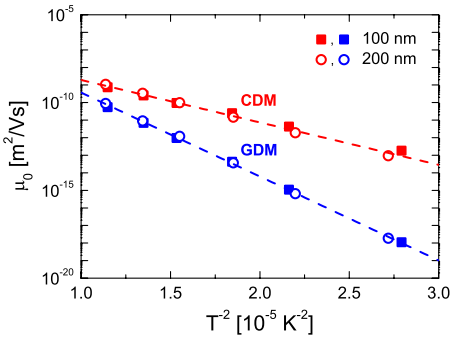

FIG. 6. (Color online) Temperature dependence of the mobility in the zero field and carrier density limit for the GDM ($\mu_{0,\mathrm{GDM}}$) and for the CDM ($\mu_{0,\mathrm{CDM}}$). The solid squares (open circles) indicate the values for the 100 (200) nm device.

as discussed already in more detail in Sec. II.

For both the GDM and the CDM, the mobility in the limit of zero field and carrier density is predicted to depend on temperature as

$$\mu_0(T) = \mu_0^* \exp\left[-C\left(\frac{\sigma}{k_B T}\right)^2\right]. \tag{5}$$

The temperature dependence of $\mu_{0,\mathrm{GDM}}$ and $\mu_{0,\mathrm{CDM}}$ is shown in Fig. 6 on a log μ versus $1/T^2$ scale. From the linear fits, C values of 0.42 ± 0.07 and 0.34 ± 0.08 are obtained for the GDM and for the CDM, respectively. The mobility in the infinite temperature limit, μ_0^*, is found to be $(2.2 \pm 0.4) \times 10^{-5}$ m^2/V s for the GDM and $(5 \pm 2) \times 10^{-7}$ m^2/V s for the CDM.

The material and device parameters that give rise to an optimal description of the $J(V)$ curves are summarized in Table I. We remark that their determination from the analysis given above is more robust than might be anticipated. Within the GDM and the CDM, the carrier density and the field dependence of the mobility depend only on shape of the DOS, specified by N_t and σ. Varying the mobility in the zero-density and zero-field limit, specified by μ_0^* and the slope s of the log μ versus $1/T^2$ fits, gives rise to an overall vertical shift of the $J(V)$ curves, but does not affect the shape. As a consequence, correlated errors could occur between μ_0^* and s, and between N_t and σ, but not between two parameters belonging to a different parameter pair. When estimating the uncertainty values given in Table I we have considered all possible correlated errors. For example, the uncertainty in s is very small, but the uncertainty in C is much larger, as it is to a large extent determined by the uncertainty in the σ-values.

TABLE I. Overview of the four GDM and CDM material parameters and of the parameters ϕ_1 and V_{bi}, related to the injection barriers, that optimally describe the experimental $J(V)$ curves. The relative permittivity ε_r of α-NPD was chosen equal to 3.8.

Parameter	GDM	CDM
N_t (10^{27} m^{-3})	0.20 ± 0.04	3.7 ± 0.8
σ (eV)	0.14 ± 0.01	0.10 ± 0.01
μ_0^* [10^{-6} m^2/(V s)]	22 ± 4	0.5 ± 0.2
C	0.42 ± 0.07	0.34 ± 0.08
ϕ_1 (eV)	0.4 ± 0.1	0.4 ± 0.1
V_{bi} (V)	1.5 ± 0.1	1.5 ± 0.1

IV. DISCUSSION

We concluded in Sec. III A that the conventional PF-type mobility model does not provide a consistent description of the $J(V)$ curves with respect to the layer thickness dependence. Therefore, we focus here on the GDM and the CDM, and investigate what could be learnt from the four parameters (N_t, σ, μ_0^*, and C, given in Table I) that describe within each model the mobility.

First, we discuss the DOS as obtained from the analyzes using the GDM and the CDM. As for disordered organic semiconductors the width of the DOS is typically observed to fall in the range 0.06–0.15 eV, the values of σ which are obtained within both models (0.10 and 0.14 eV) are physically realistic. Lacking independent experimental information on the width of the DOS, the values of σ can presently not be used to make a distinction between both models. However, it is possible to make such a distinction from the values obtained for the site density. For the GDM, the highest N_t value allowed within the uncertainty margins is still more than five times lower than the experimentally determined density of α-NPD molecules, 1.4×10^{27} m^{-3}. On the other hand, for the CDM the lowest N_t value allowed within the uncertainty margins is only ~ 2 times larger. We view this as an indication that for α-NPD the energies of the sites in between which hopping takes place are correlated. The factor ~ 2 difference between the N_t values as obtained from the fit and as obtained from the chemical analysis could tentatively be explained by considering that each α-NPD molecule consists of two equivalent triarylamine units, each contributing one HOMO state. Substantial torsion around the central bond in the molecule could lead to a reduction in the hybridization between both states, giving rise to two almost degenerate energy levels which are each localized predominantly on one of the two triarylamine units. Results of electronic structure calculations by Zhang *et al.*[70] support this picture. The molecular configuration with the two parts of the molecule rotated 90° around the central C–C bond was found to be energetically most favorable. This implies that the interaction between the two HOMO states, found to be localized on the two N-atoms, is very weak.

The site-energy correlations in disordered small molecule materials might originate from the deposition process. It is plausible that a molecule approaching the surface of the (growing) α-NPD layer during low-temperature evaporation deposition in vacuum tends to search for an energetically favorable "docking spot."[71] As the local HOMO and LUMO levels of the individual molecules are expected to be strongly affected by molecule-molecule interactions, depending on the distance and relative orientation of the molecules, the HOMO and LUMO levels of neighboring molecules might be expected to be correlated. This ordering process might be less efficient in the case of polymer systems, due to the length of the molecules and the reduced mobility of the molecules induced by the use of side chains.

Second, we investigate the mobility in the zero-density and zero-field limit, which is described by the parameters μ_0^* and C using Eq. (5). Both parameters are clearly defined within the scope of the GDM and the CDM, within which the Miller–Abrahams[72] approximation is used for expressing the hopping rate

$$\nu(r,\Delta E) = \nu_0 \exp(-2\alpha r)\exp\left(-\frac{|\Delta E| + \Delta E}{2k_B T}\right), \quad (6)$$

as a function of the intersite distance r and the energy difference ΔE between the final and initial state. Here ν_0 is an attempt frequency and α^{-1} is the extension of the wave functions in between which the hopping takes place. The parameter C, which describes the temperature dependence of the mobility in the zero-field and zero-density limit, is known from percolation theory to depend (weakly) on α^{-1}. An increase in the localization (decrease in the wave function extension) leads to an enhanced contribution to the conductivity of thermally excited hops (and a decreased role of nonactivated long-distance tunneling processes), resulting in an increase in C. For the GDM, C values in the range 0.38–0.46 are expected,[11,73] depending on the value of α, with $C=0.42$ for $\alpha^{-1}=0.1\times a$. For the CDM, $C\cong 0.36$ is then expected from Monte Carlo calculations,[18] whereas a value of $C\cong 0.29$ has been obtained from 3D-ME calculations.[19] The values as obtained within the GDM and the CDM are consistent with the values expected theoretically. Therefore, we regard these for both models as physically realistic.

The parameter μ_0^* is the mobility in the zero-field, zero-density, and high-temperature limit, and is given by $\mu_0^* \cong a^2 e \nu_0'/\sigma$,[13,19] where $a \equiv (N_t)^{1/3}$ is the average intersite distance and where $\nu_0' \equiv \nu_0 \exp(-2\alpha a)$ is the average hopping rate between equal-energy nearest neighbor sites. The parameter values listed in Table I yield $\nu_0' \cong 1.1\times 10^{12}$ s^{-1} and $\nu_0' \cong 1.2\times 10^{11}$ s^{-1} for the GDM and the CDM, respectively. An oversimplified picture would suggest that the attempt frequency is of the order of a typical vibrational frequency, $\sim 10^{13}$ s^{-1}, which is evidently larger than the values of ν_0' obtained. However, microscopic-scale modeling such as reviewed in Ref. 74 will be needed for establishing a relationship between the effective value of ν_0' (and of α), the intersite transfer integral distribution and the effective structural reorganization energies involved upon charge transfer.

The wide spread in zero-field hole mobilities reported in the literature for α-NPD can be explained in several ways. It could originate from different degrees of purity of the organic material and from a neglect or improper treatment in the analysis of the effect of the injection barrier. It could also be explained within the framework of the GDM or CDM, as the mobility in disordered organic materials is density dependent, the (effective) mobility as determined in a thick device (with a small average hole density) is expected to be lower than the mobility as determined in a thin device (with a larger average hole density).[62] In a similar way it may be explained why the values of σ found in the literature are in almost all cases somewhat smaller (0.05–0.08 eV in Refs 43, 47, and 48, but up to 0.12 eV in Ref. 24) than the value of 0.10 eV in our work, obtained using the CDM. The *effective* temperature dependence of the mobility obtained when (incorrectly) neglecting the carrier density dependence of the mobility is smaller than in the zero density limit, therefore leading to a smaller effective value of σ. In order to be able to make an in-depth comparison with results obtained from various transient techniques, such as time-of-flight or impedance measurements, it would be necessary to extend the analysis of the results as obtained from these techniques to include the carrier density dependence of the mobility.

V. SUMMARY AND CONCLUSIONS

For the first time, charge transport in a small molecule material has been investigated in the frameworks of the GDM and the CDM while taking the effects of the carrier density dependence of the mobility due to the disorder into account. It is found that an excellent and fully consistent description of the voltage, thickness, and temperature dependence of the current density in α-NPD hole-only devices can be obtained within both models, and that also the temperature dependence of the mobility in the zero field and carrier density limit, μ_0, has the proper $1/T^2$ dependence as predicted from theory. Whereas the analysis with the GDM and with the CDM lead to a fully consistent description, an analysis of the same extended set of $J(V)$ curves using the conventional PF-type field-dependent mobility did not lead to a consistent description of the $J(V)$ curves for all layer thicknesses studied.

In contrast to recent findings for two types of polymers used in OLEDs, discussed in Sec. I, we conclude that evidence has been provided that in the small molecule material α-NPD the site energies are correlated. This is suggested by the observation that the site density as obtained from the analysis of the current-voltage curves is much closer to the experimentally determined molecule volume density in the case of the CDM than for the case of the GDM. Establishing the presence of spatially correlated disorder is expected to be a crucial step toward building up predictive OLED device models.

ACKNOWLEDGMENTS

We would like to thank A. J. M. van den Biggelaar for skilful sample preparation, and A. C. A. Jonkers, T. J. M. Verspaget, C. Hermans, and J. Smulders for carrying out the ICP-AES measurements. This research has received funding from the Dutch nanotechnology program NanoNed (contribution S.L.M.v.M.), and from the European Community's Program No. FP7-213708 (AEVIOM, contribution R.C.).

[1] B. W. D'Andrade and S. R. Forrest, Adv. Mater. **16**, 1585 (2004).
[2] K. Walzer, B. Maennig, M. Pfeiffer, and K. Leo, Chem. Rev. **107**, 1233 (2007).
[3] J. K. F. So and P. Burrows, MRS Bull. **33**, 663 (2008).
[4] S. Reineke, F. Lindner, G. Schwartz, N. Seidler, K. Walzer, B. Lüssem, and K. Leo, Nature (London) **459**, 234 (2009).
[5] S. R. Forrest, Nature (London) **428**, 911 (2004).
[6] H. Böttger and V. V. Bryksin, *Hopping Conduction in Solids* (Akademie-Verlag, Berlin, 1985).
[7] H. Bässler, Phys. Status Solidi B **175**, 15 (1993).
[8] S. D. Baranovskii, T. Faber, F. Hensel, and P. Thomas, J. Phys.: Condens. Matter **9**, 2699 (1997); S. D. Baranovskii, H. Cordes, F. Hensel, and G. Leising, Phys. Rev. B **62**, 7934 (2000); O. Rubel, S. D. Baranovskii, P. Thomas, and S. Yamasaki, *ibid.* **69**, 014206 (2004).

[9]V. I. Arkhipov, P. Heremans, E. V. Emelianova, G. J. Adriaenssens, and H. Bässler, J. Phys.: Condens. Matter **14**, 9899 (2002).
[10]Y. Roichman and N. Tessler, Synth. Met. **135–136**, 443 (2003); Y. Roichman, Y. Preezant, and N. Tessler, Phys. Status Solidi A **201**, 1246 (2004).
[11]R. Coehoorn, W. F. Pasveer, P. A. Bobbert, and M. A. J. Michels, Phys. Rev. B **72**, 155206 (2005).
[12]I. I. Fishchuk, V. I. Arkhipov, A. Kadashchuk, P. Heremans, and H. Bässler, Phys. Rev. B **76**, 045210 (2007).
[13]W. F. Pasveer, J. Cottaar, C. Tanase, R. Coehoorn, P. A. Bobbert, P. W. M. Blom, D. M. de Leeuw, and M. A. J. Michels, Phys. Rev. Lett. **94**, 206601 (2005).
[14]J. Zhou, Y. C. Zhou, J. M. Zhao, C. Q. Wu, X. M. Ding, and X. Y. Hou, Phys. Rev. B **75**, 153201 (2007).
[15]P. M. Borsenberger and D. S. Wiess, *Organic Photoreceptors for Xerography* (Marcel Dekker, New York, 1998).
[16]W. Brütting, S. Berleb, and A. G. Mückel, Org. Electron. **2**, 1 (2001).
[17]Y. N. Gartstein and E. M. Conwell, Chem. Phys. Lett. **245**, 351 (1995).
[18]S. V. Novikov, D. H. Dunlap, V. M. Kenkre, P. E. Parris, and A. V. Vannikov, Phys. Rev. Lett. **81**, 4472 (1998).
[19]M. Bouhassoune, S. L. M. van Mensfoort, P. A. Bobbert, and R. Coehoorn, Org. Electron. **10**, 437 (2009).
[20]In Ref. 19 the model descriptions of the mobility obtained was labled as "ECDM," emphasizing the extension of the model description to include the charge carrier density dependence. However, as the underlying disorder model was not changed, we avoid here any possible confusion and refer to this work as "CDM." Similarly we refer to the work presented in Ref. 13 as "GDM."
[21]G. Malliaras, Y. Shen, D. H. Dunlap, H. Murata, and Z. H. Kafafi, Appl. Phys. Lett. **79**, 2582 (2001).
[22]M. A. Baldo and S. R. Forrest, Phys. Rev. B **64**, 085201 (2001).
[23]D. Poplavskyy and J. Nelson, J. Appl. Phys. **93**, 341 (2003).
[24]T.-Y. Chu and O.-K. Song, J. Appl. Phys. **104**, 023711 (2008).
[25]A. Ohno, A. Haruyama, K. Kurotaki, and J.-I. Hanna, J. Appl. Phys. **102**, 083711 (2007).
[26]C. Tanase, P. W. M. Blom, and D. M. de Leeuw, Phys. Rev. B **70**, 193202 (2004).
[27]Y. Nagata and C. Lennartz, J. Chem. Phys. **129**, 034709 (2008).
[28]W. Gao and A. Kahn, J. Appl. Phys. **94**, 360 (2003).
[29]S. A. Van Slyke, C. H. Chen, and C. W. Tang, Appl. Phys. Lett. **69**, 2160 (1996).
[30]M. A. Baldo, S. Lamansky, P. E. Burrows, M. E. Thomson, and S. R. Forrest, Appl. Phys. Lett. **75**, 4 (1999).
[31]R. S. Deshpande, V. Bulovic, and S. R. Forrest, Appl. Phys. Lett. **75**, 888 (1999).
[32]J.-W. Kang, D.-S. Lee, H.-D. Park, J. W. Kim, W.-I. Jeong, Y.-S. Park, S.-H. Lee, K. Gob, J.-S. Lee, and J.-J. Kim, Org. Electron. **9**, 452 (2008).
[33]K. S. Son, M. Yahiro, T. Imai, H. Yoshizaki, and C. Adachi, Chem. Mater. **20**, 4439 (2008).
[34]Q. Wang, J. Ding, Z. Zhang, D. Ma, Y. Cheng, L. Wang, and F. Wang, J. Appl. Phys. **105**, 076101 (2009).
[35]S. Lee, C.-H. Chung, and S. M. Cho, Synth. Met. **126**, 269 (2002).
[36]Y. Kijima, A. Nobutoshi, and S. Tamura, Jpn. J. Appl. Phys., Part 1 **38**, 5274 (1999).
[37]T. Tsuji, S. Naka, H. Okada, and H. Onnagawa, Appl. Phys. Lett. **81**, 3329 (2002).
[38]K. O. Cheon and J. Shinar, Appl. Phys. Lett. **81**, 1738 (2002).
[39]M. Nakahara, M. Minagawa, T. Oyamada, T. Tadokoro, H. Sasabe, and C. Adachi, Jpn. J. Appl. Phys., Part 2 **46**, L636 (2007).
[40]R. Meerheim, S. Schoolz, S. Olthof, G. Schwartz, S. Reineke, K. Waltzer, and K. Leo, J. Appl. Phys. **104**, 014510 (2008).
[41]T. Matsushima and C. Adachi, Thin Solid Films **517**, 874 (2008).
[42]T. Matsushima, Y. Kinoshita, and H. Murata, Appl. Phys. Lett. **91**, 253504 (2007).
[43]P. M. Borsenberger, E. H. Mangin, and J. Shi, Physica B **217**, 212 (1996).
[44]Z. Deng, S. T. Lee, D. P. Webb, Y. C. Chan, and W. A. Gambling, Synth. Met. **107**, 107 (1999).
[45]S. Naka, H. Okada, H. Onnagawa, Y. Yamaguchi, and T. Tsutsui, Synth. Met. **111–112**, 331 (2000).
[46]W. Weise, T. Keith, N. von Malm, and H. von Seggern, Phys. Rev. B **72**, 045202 (2005).
[47]A. Fleissner, H. Schmidt, C. Melzer, and H. von Seggern, Appl. Phys. Lett. **91**, 242103 (2007).
[48]K. L. Tong, S. W. Tsang, K. K. Tsung, S. C. Tse, and S. K. So, J. Appl. Phys. **102**, 093705 (2007).
[49]C.-Y. Lin, Y.-M. Chen, H.-F. Chen, F.-C. Fang, Y.-C. Lin, W.-Y. Hung, K. T. Wong, R. C. Kwong, and S. C. Xia, Org. Electron. **10**, 181 (2009).
[50]N. D. Nguyen, M. Schmeits, and H. P. Loebl, Phys. Rev. B **75**, 075307 (2007).
[51]S. L. M. van Mensfoort, S. I. E. Vulto, R. A. J. Janssen, and R. Coehoorn, Phys. Rev. B **78**, 085208 (2008).
[52]R. J. de Vries, S. L. M. van Mensfoort, V. Shabro, R. A. J. Janssen, and R. Coehoorn, Appl. Phys. Lett. **1094**, 163308 (2009).
[53]Y.-J. Cheng, M. S. Liu, Y. Zhang, Y. Niu, F. Huang, J.-W. Ka, H.-L. Yip, Y. Tian, and A. K.-Y. Jen, Chem. Mater. **20**, 413 (2008).
[54]A. Wan, J. Hwang, F. Amy, and A. Kahn, Org. Electron. **6**, 47 (2005).
[55]S. L. M. van Mensfoort and R. Coehoorn, Phys. Rev. Lett. **100**, 086802 (2008).
[56]N. Koch, A. Kahn, J. Ghijsen, J.-J. Pireaux, J. Schwartz, R. L. Johnson, and A. Elschner, Appl. Phys. Lett. **82**, 70 (2003).
[57]H. Ishii, K. Sugiyama, E. Ito, and K. Seki, Adv. Mater. **11**, 605 (1999).
[58]A. Kahn, N. Koch, and W. Gao, J. Polym. Sci., Part B: Polym. Phys. **41**, 2529 (2003).
[59]C. Tengstedt, W. Osikowicz, W. Salaneck, I. D. Parker, C.-H. Hsu, and M. Fahlman, Appl. Phys. Lett. **88**, 053502 (2006).
[60]E. H. Evans, J. A. Day, C. D. Palmer, C. M. M. Smith, and M. M. Clare, J. Anal. At. Spectrom. **24**, 711 (2009).
[61]W. D. Gill, J. Appl. Phys. **43**, 5033 (1972).
[62]S. L. M. van Mensfoort and R. Coehoorn, Phys. Rev. B **78**, 085207 (2008).
[63]For a more elaborate description of the calculation of the error we refer to Ref. 52.
[64]S. J. Martin, J. M. Lupton, I. D. W. Samuel, and A. B. Walker, J. Phys.: Condens. Matter **14**, 9925 (2002).
[65]N. I. Craciun, J. Wildeman, and P. W. M. Blom, Phys. Rev. Lett. **100**, 056601 (2008).
[66]S. V. Rakhmanova and E. M. Conwell, Appl. Phys. Lett. **76**, 3822 (2000).
[67]Z. G. Yu, D. L. Smith, A. Saxena, R. L. Martin, and A. R. Bishop, Phys. Rev. Lett. **84**, 721 (2000).
[68]S. V. Novikov and A. V. Vannikov, J. Phys. Chem. **99**, 14573 (1995).
[69]P. R. Emtage and J. J. O'Dwyer, Phys. Rev. Lett. **16**, 356 (1966).
[70]R. Q. Zhang, C. S. Lee, and S. T. Lee, J. Chem. Phys. **112**, 8614 (2000).
[71]J. J. Kwiatkowski, J. Nelson, H. Li, J. L. Bredas, W. Wenzel, and C. Lennartz, Phys. Chem. Chem. Phys. **10**, 1852 (2008).
[72]A. Miller and E. Abrahams, Phys. Rev. **120**, 745 (1960).
[73]S. D. Baranovskii, I. P. Zvyagin, H. Cordes, S. Yamasaki, and P. Thomas, Phys. Status Solidi B **230**, 281 (2002).
[74]V. Coropceanu, J. Cornil, D. A. da Silva Filho, Y. Olivier, R. Silbey, and J.-L. Bredas, Chem. Rev. **107**, 926 (2007).